von Kummer et al., 1994; Krieger et al., 1999; Manelfe et al., 1999; Marks et al., 1999; Bozzao et al., 1989). However, the relationship between these findings and patient prognosis remains controversial (Leys et al., 1992; Moulin et al., 1996; Büttner et al., 1997; von Kummer et al., 1994; Krieger et al., 1999; Hénon et al., 1995). On the other hand, the baseline score of the National Institute of Health Stroke Scale (NIHSS) is widely used as a rating instrument to measure neurologic deficits and predict outcome after stroke (Krieger et al., 1999; Adams et al., 1999; DeGraba et al., 1999; Muir et al., 1996). A baseline NIHSS score of ≥ 16 suggests a high probability of death or severe disability whereas a score of ≤ 6 predicts a good recovery (Adams et al., 1999).

While intra-arterial angiography and magnetic resonance angiography (MRA) provide substantial information about occlusive lesions in cerebral arteries, these methods may not be readily available. Neurosonologic examination provides a convenient, relatively inexpensive, method that can be performed in real time at the bedside. Therefore, we investigated findings of carotid ultrasonography, brain CT, and baseline NIHSS score within 6 h of stroke onset, and examined which one of these parameters most strongly predicts the likelihood of patient prognosis 1 month after stroke onset.

2. Materials and methods

Out of 253 consecutive patients with carotid acute ischemic stroke or TIA within 7 days after stroke onset admitted to our hospital between January 1997 and April 1999, 82 patients were admitted within 6 h. Nine patients were excluded because of a disability due to previous stroke ($n = 5$) or a superselective intraarterial thrombolytic therapy ($n = 4$). Therefore, we enrolled 73 patients (53 men and 20 women; age 71.0 ± 10.9 years) into this study. Stroke subtype was atherothrombotic brain infarction in 12, cardioembolic stroke in 30, lacunar infarction in 12, and other in ten and TIA in nine patients. They were all examined by both brain CT and duplex carotid ultrasonography within 6 h of stroke onset.

Early CT findings were defined as obscuration of the lentiform nucleus, loss of the insular ribbon and/or cortical effacement. The CT findings were determined by the consensus of two experienced neurologists (M. Koga and K. Kimura).

US examination was performed using an Advanced Technology Laboratories Ultramark 9 HDI (ATL, Bothell, WA) with a linear-array transducer operating at 5.0–10.0 MHz. The pulse repetition frequency was primarily 5000 Hz, and the low-pass filter was 50 Hz. Imaging was performed while the subjects were lying in the supine position with the head turned away from the side being scanned and neck extended. The ICA origin and the common carotid artery (CCA) were examined in the longitudinal and transverse planes with anterior, lateral, and posterior approaches using B-mode, color Doppler, power Doppler and pulse Doppler. At first, we evaluated the degree of ICA stenosis. We measured the degree of diameter stenosis in longitudinal views. The diameter of the stenosis was calculated as $1 - (r/n) \times 100$, where r is the diameter of the residual lumen and n is the diameter of normal vessel at the level of the stenosis. When color Doppler or power Doppler shown the degree of ICA stenosis $>$ 50%, we measured the highest peak-systolic blood flow velocity (PSV) in stenotic lesions using pulse Doppler. The velocities were corrected by the incidence angle. We identified the PSV greater than 200 cm/s as ICA stenosis greater than 70% (Koga et al., 2001). Second, we evaluated the blood flow velocity of the CCA on longitudinal scans. A sample volume 5–7 mm in size was set in the CCA, which were displayed as linearly possible. Special care was taken to keep the incident angle between the CCA and the beam at 30–60°, and the velocities were corrected by the incidence angle. We measured the end diastolic velocity in the CCA and calculated the side-to-side ratio of the end-diastolic flow velocity in the CCA (ED ratio). US findings were considered positive when the PSV of ICA was >200 cm/s and/or the ED ratio exceeded 1.4, indicating probable ICA or middle cerebral artery trunk (M1) occlusion (Kimura et al., 1997; Yasaka et al., 1992).

The NIHSS score (Brott et al., 1989) at admission and modified Rankin scale score (van Swieten et al., 1988) on day 30 were evaluated. The NIHSS is a graded neurological examination rating speech and language, cognition, visual field deficits, motor and sensory impairments, and ataxia. The modified Rankin scale is a simple graded examination of disability in stroke patients. Death was represented as a modified Rankin scale score of six. The following clinical characteristics were analyzed: age (years), sex, angiographic findings (digital subtraction angiography (DSA, $n = 24$) or magnetic resonance angiography (MRA, $n = 30$)) within 2 weeks after stroke onset, risk factors of cerebrovascular disease (including hypertension, diabetes mellitus, hypercholesterolemia, atrial fibrillation and cigarette smoking) and mortality. The following risk factors were identified: (1) use of antihypertensive agents or blood pressure recordings before onset with systolic blood pressure ≥ 160 mmHg or diastolic blood pressure ≥ 95 mmHg for hypertension; (2) use of insulin or oral hypoglycemic agents, fasting blood glucose ≥ 140 mg/dl, or random blood glucose ≥ 200 mg/dl for diabetes mellitus; (3) use of antilipotropic agents, or total cholesterol on admission ≥ 220 mg/dl for hypercholesterolemia.

We classified patients into four groups: Group 1, with negative CT findings and negative US findings; Group 2, with negative CT findings and positive US findings; Group 3, with early CT findings and negative US findings; Group 4, with early CT findings and positive US findings. We compared the groups and analyzed predictors to determine poor outcome. We considered a modified Rankin scale score of ≥ 3 to be a poor outcome and NIHSS score of ≥ 16 as a predictive variable for poor outcome (Adams et al., 1999).

In 54 patients evaluated by DSA or MRA, we calculated the sensitivity, specificity, positive predictive value, negative predictive value and accuracy of US findings, to predict angiographic ICA or M1 occlusion, or severe stenosis of ICA.

We used STATVIEW 5.0 software (Abacus Concepts Inc., Berkeley, CA) for statistical analysis. Age is presented as mean $\pm$ S.D. Groups were compared in terms of baseline NIHSS score, modified Rankin scale score on day 30 using the Kruskal–Wallis test. The NIHSS score and modified Rankin scale score are represented as the median (range). We further analyzed the relationship between patient outcome and carotid US findings combined with a baseline NIHSS ≥ 16, early CT findings and other factors. In the univariate analysis, categorical variables were compared by the χ^2-test, continuous variables were compared by unpaired Student's t-test, and scoring variables were compared using the Kruskal–Wallis test. Multivariate analysis was performed by logistic regression to identify the predictor variables for poor outcome (modified Rankin scale score ≥ 3). Differences were considered significant at $P < 0.05$.

3. Results

Positive US findings were observed in 33 patients; ED ratio over 1.4 in 27 patients and ICA stenosis greater than 70% in six patients. Eighteen out of 27 patients with an ED ratio over 1.4 were examined by DSA ($n = 10$) or MRA ($n = 8$), which demonstrated ICA occlusion in 11 patients, M1 occlusion in four, 90% stenosis of the carotid ICA in 1, M1 severe stenosis in one and normal findings in one patient. ICA stenosis $> 70\%$ was confirmed in four out of six patients by DSA ($n = 1$) or MRA ($n = 3$). In the remaining 40 patients with negative US findings, 32 patients were evaluated by DSA ($n = 13$) or MRA ($n = 19$). Angiography presented normal findings in 25 patients, M2 occlusion in three, severe M1 stenosis in two, severe stenosis of the distal ICA in one, and occlusion of the anterior cerebral artery (ACA) in one patient. In 54 patients evaluated by DSA or MRA, using the angiographic findings as the gold standard, sensitivity was 95.2%, specificity was 93.9%, positive predictive value was 90.9%, negative predictive value was 96.9% and accuracy of US findings to predict ICA or M1 occlusion, or severe stenosis of ICA was 94.4%.

Early CT findings were observed in 22 patients; obscuration of the lentiform nucleus only in eight, loss of insular ribbon in one, effacement of the cortex only in three, both obscuration of the lentiform nucleus and loss of insular ribbon in

two, both obscuration of the lentiform nucleus and effacement of the cortex in two, both loss of insular ribbon and effacement of the cortex in one, and all findings in five patients.

Thirty patients were affected on the right side, 40 on the left side and three patients were affected bilaterally. Risk factors of cerebrovascular disease, included 52 cases of hypertension (71.2%), 18 diabetes mellitus (24.7%), 23 hypercholesterolemia (31.5%), 25 atrial fibrillation (34.2%), 22 other cardiac diseases (ischemic heart disease, cardiomyopathy, heart failure, mitral valve disease and patent foramen ovale, 30.1%) and 39 smoking (53.4%).

The median baseline NIHSS score was 8 (0–31) and median modified Rankin scale score on day 30 was 1 (0–6). Six patients died within 1 month of stroke onset.

Table 1 shows the clinical characteristics of the four groups. The age in Group 2 was higher than that in Group 1 and Group 4. No differences in other characteristics observed among four groups. NIHSS score at admission was in descending order Group 4 (18 [9–25]) > Group 3 (12 [3–22]) > Group 2 (7.5 [2–31]) > Group 1 (5 [0–13]) ($P < 0.0001$, Kruskal–Wallis test) and was more strongly related to CT findings than US findings (Table 2). The relationship between the groups and categorized baseline NIHSS score is shown in Fig. 1. On the other hand, the modified Rankin

Table 1
Patients' characteristics of four groups

	Group 1 ($n = 35$)	Group 2 ($n = 16$)	Group 3 ($n = 5$)	Group 4 ($n = 17$)	P
Age (year)[a]	68.3 ± 10.9	77.7 ± 9.2[b]	72.2 ± 10.2	69.6 ± 10.7	0.035[c]
Male (%)	77	81	60	59	NS[d]
Risk factor (%)					
Hypertension	63	81	100	71	NS[d]
Diabetes mellitus	17	38	60	18	NS[d]
Hypercholesterolemia	37	25	40	24	NS[d]
Atrial fibrillation	31	25	80	35	NS[d]
Disease	23	25	40	47	NS[d]
Smoking	60	63	60	29	NS[d]

Group 1, patients with negative CT findings and negative US findings. Group 2, patients with negative CT findings and positive US findings. Group 3, patients with early CT findings and negative US findings. Group 4, patients with early CT findings and positive US findings.

[a] Average ± S.D.

[b] Higher than Group 1 and 4. NS, indicates not significant.

[c] χ^2-Test.

[d] One way analysis of variance (ANOVA).

Table 2
NIHSS score and modified Rankin scale score

	Group 1 ($n = 35$)	Group 2 ($n = 16$)	Group 3 ($n = 5$)	Group 4 ($n = 17$)	P
NIHSS score at admission[a]	5 (0–13)	7.5 (2–31)	12 (3–22)	18 (9–25)	<0.0001[b]
Modified Rankin scale score on day 30[a]	0 (0–5)	2.5 (0–6)	1 (0–2)	4 (0–6)	<0.0001[b]

Group 1, patients with negative CT findings and negative US findings. Group 2, patients with negative CT findings and positive US findings. Group 3, patients with early CT findings and negative US findings. Group 4, patients with early CT findings and positive US findings.

[a] Median (range).

[b] Kruskal–Wallis test.

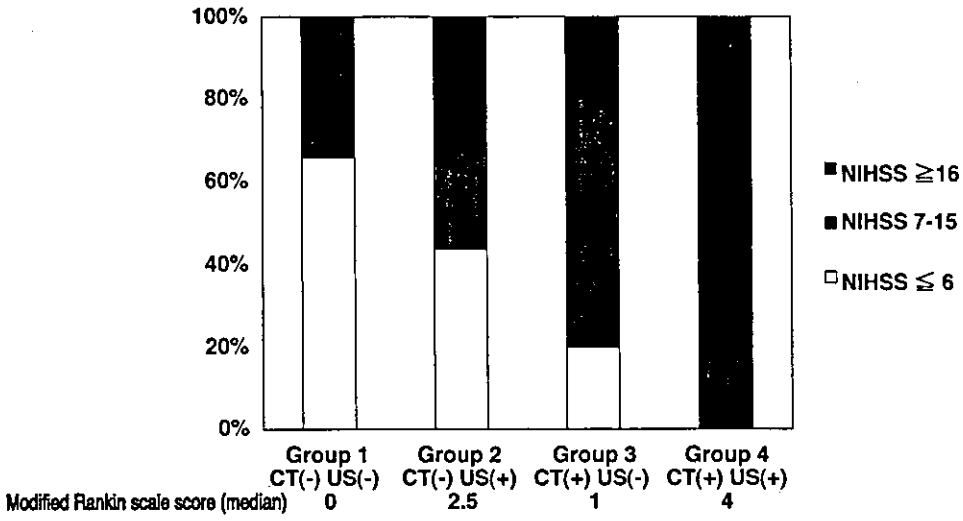

Fig. 1. Baseline NIHSS score.

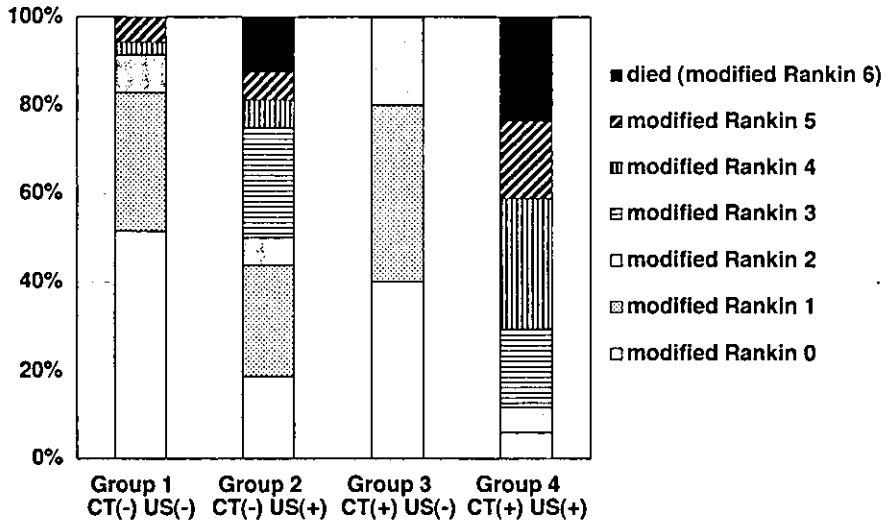

Fig. 2. Modified Rankin scale score on 30 days.

score on day 30 was in descending order: Group 4 (4 [range 0–5]) > Group 2 (2.5 [0–6]) > Group 3 (1 [0–2]) and 1 (0 [range 0–6]) ($P < 0.0001$) and was more strongly related to US findings than CT findings (Table 2 and Fig. 2). There were no stroke deaths in Group 1 or 3, two stroke deaths in Group 2 (13%) and four stroke deaths in Group 4 (24%).

According to univariate analysis, age ($P = 0.011$), NIHSS ≥ 16 ($P < 0.0001$), early CT findings ($P = 0.0001$), and positive US findings ($P < 0.0001$) were all significant predictors of a poor outcome (Table 3).

According to multiple logistic regression analysis, age (by year, $P = 0.041$, odds ratio = 1.1), baseline NIHSS score ≥ 16 ($P = 0.036$, odds ratio, 7.9), and positive US findings ($P = 0.0045$, odds ratio, 11.1) were independent predictors of a poor outcome (Table 4).

4. Discussion

Moulin et al. (1996) suggested that CT could provide a simple tool in evaluating the early prognosis of MCA infarction. Studies have shown that MCA hypodensity of more than 33% within 6 h of stroke onset correlates with poor outcome (Marks et al., 1999), and MCA hypodensity of more than 50% within 6 h of onset represent a high risk for developing fatal brain swelling (Krieger et al., 1999). Moulin et al. further suggested that the presence of two or three early CT findings (obscuration of the lentiform nucleus, loss of the insular ribbon, or cortical effacement) is associated with a poor outcome. In our study, the presence of two or three early CT findings was observed in ten cases. When we analyzed the relationship between the presence of two or three early CT findings and patients' outcome, two or three early CT findings did not represent an independent predictor of poor outcome according to multiple regression analysis ($P = 0.31$). On the other hand, age (by year, $P = 0.047$, odds ratio, 1.1), NIHSS score ≥ 16 ($P = 0.041$, odds ratio, 7.9) and positive US findings ($P = 0.0048$, odds ratio, 10.2) were independent predictors of a poor outcome. Our results suggested that US findings are superior to positive CT findings.

Table 3
Univariate analysis of variables by modified Rankin scale score

	Modified Rankin scale score		P
	≤ 2 ($n = 47$)	≥ 3($n = 26$)	
Age (year)	68.6 ± 9.8	75.3 ± 11.7	<0.05[a]
Male (%)	79	62	NS[b]
NIHSS ≥ 16 (%)	4	62	<0.0001[b]
Early CT findings (%)	15	58	0.0001[b]
Positive US findings (%)	21	88	<0.0001[b]

[a] Unpaired Student's t-test.
[b] χ^2-Test. NS, indicates not significant.

Table 4
Multiple logistic regression analysis of variables by modified Rankin scale score

	Odds ratio	95% CI	P
Age (by year)	1.1	1.0–1.2	<0.05
NIHSS ≥ 16	7.9	1.1–54.7	<0.05
Early CT findings	3.4	0.6–19.5	NS[a]
Positive US findings	11.1	2.1–58.5	<0.005

[a] NS, indicates not significant.

The NIHSS score is a widely used rating instrument to measure neurologic deficits. In a recent study comparing several stroke scales, NIHSS demonstrated excellent specificity, sensitivity and accuracy in predicting patients' outcome (Muir et al., 1996). Adams et al. (1999) reported that a baseline NIHSS score of ≥ 16 is predictive of a high probability of death or severe disability whereas a score of ≤ 6 is predictive of a good recovery. Therefore, in the present study, we used a baseline NIHSS ≥ 16 as the variable to predict poor outcome. However, our results demonstrated that positive US findings are superior to a baseline NIHSS score ≥ 16 to predict patients' outcome.

Camerlingo et al. (1996) suggested that US examinations would be useful in the management of acute carotid stroke as an early indicator of patients with a worse prognosis. Patients with ischemic stroke within the first 6 h who had intracranial (ICA or M1) occlusion and scarce or absent collateral filling at early angiography, had the worst clinical outcome (Fieschi et al., 1989). The mortality rate of patients with ICA occlusion is high, due to brain edema which is often fatal (Oxbury et al., 1975; Heinsius et al., 1998). In studies of thrombolytic therapy, poor outcome or death was also associated with ICA occlusion (Jansen et al., 1995; Jahan et al., 1999; Urbach et al., 1997). Thus, arterial pathological lesions such as ICA occlusion or severe stenosis, may represent a very reliable predictor of patient's outcome. Our study demonstrated that the US diagnosis for occlusive arterial lesions was nearly completed. Therefore, US findings may provide a very strong predictive tool for patients' outcome.

One patient had normal angiographic findings but an ED ratio > 1.4. The majority of patients who had DSA or MRA carried out US examinations before angiographic evaluations. The re-

canalization of an occluded artery may explain the discrepancy of the results between two studies.

Intravenous thrombolysis with tissue plasminogen activator (t-PA) given within 3 h of stroke onset improves long-term outcome (The National Institute of Neurological Disorders and Stroke rt-PA Stroke Study Group, 1995). Neurosonologic examination may, therefore, be useful to evaluate occlusive lesions in cerebral arteries immediately before thrombolytic therapy in acute stroke patients. The outcome of almost all patients of our Group 1 and three patients with negative US findings was good. Based on these findings, thrombolytic therapy may not be indicated for Group 1 and three patients. Recanalization could not be achieved through early thrombolytic treatment in most cases of occluded ICA (Boysen et al., 1996). On the other hand, t-PA should be indicated for Group 2 or four patients without ICA occlusion.

5. Summary

Positive US findings suggesting ICA or M1 occlusion, or ICA severe stenosis of hyper-acute ischemic stroke or TIA appear to provide valuable predictive tools for determining patients' outcome and are superior to early CT findings and baseline NIHSS.

Acknowledgements

This work was supported in part by the Research Grant for Cardiovascular Disease (12A-2) from the Ministry of Health and Welfare of Japan, and by the Special Coordination Funds for Promoting Science and Technology (Strategic Promotion System for Brain Science) from the Science and Technology Agency of Japan.

References

Adams HP Jr, Davis PH, Leira EC, Chang KC, Bendixen BH, Clarke WR, Woolson RF, Hansen MD. Baseline NIH Stroke Scale score strongly predicts outcome after stroke: a report of the Trial of Org 10172 in Acute Stroke Treatment (TOAST). Neurology 1999;53:126–31.

Bastianello S, Pierallini A, Colonnese C, Brughitta G, Angeloni U, Antonelli M, Fantozzi LM, Fieschi C, Bozzao L. Hyperdense middle cerebral artery CT sign. Comparison with angiography in the acute phase of ischemic supratentorial infarction. Neuroradiology 1991;33:207–11.

Boysen G. Fourth international symposium on thrombolytic therapy in acute ischemic stroke, Copenhagen, May 30–June 1. Cerebrovasc Dis 1996;6:175–94 Abstract.

Bozzao L, Bastianello S, Fantozzi LM, Angeloni U, Argentino C, Fieschi C. Correlation of angiographic and sequential CT findings in patients with evolving cerebral infarction. Am J Neuroradiol 1989;10:1215–22.

Brott T, Adams HP Jr, Olinger CP, Marler JR, Barsan WG, Biller J, Spilker J, Holleran R, Eberle R, Hertzberg V. Measurements of acute cerebral infarction: a clinical examination scale. Stroke 1989;20:864–70.

Büttner TH, Uffmann M, Günes N, Köster O. Early CCT signs of supratentorial brain infarction: clinico-radiological correlations. Acta Neurol Scand 1997;96:317–23.

Camerlingo M, Casto L, Censori B, Servalli MC, Ferraro B, Mamoli A. Prognostic use of ultrasonography in acute non-hemorrhagic carotid stroke. Ital J Neurol Sci 1996;17:215–8.

DeGraba TJ, Hallenbeck JM, Pettigrew KD, Dutka AJ, Kelly BJ. Progression in acute stroke: value of the initial NIH stroke scale score on patient stratification in future trials. Stroke 1999;30:1208–12.

Fell G, Phillips DJ, Chikos PM, Harley JD, Thiele BL, Strandness DE Jr. Ultrasonic duplex scanning for disease of the carotid artery. Circulation 1981;64:1191–5.

Fieschi C, Argentino C, Lenzi GL, Sacchetti ML, Toni D, Bozzao L. Clinical and instrumental evaluation of patients with ischemic stroke within the first 6 h. J Neurol Sci 1989;91:311–21.

Heinsius T, Bogousslavsky J, van Melle G. Large infarcts in the middle cerebral artery territory: etiology and outcome patterns. Neurology 1998;50:341–50.

Hénon H, Godefroy O, Leys D, Mounier-Vehier F, Lucas C, Rondepierre P, Duhamel A, Pruvo JP. Early predictors of death and disability after acute cerebral ischemic event. Stroke 1995;26:392–8.

Hoshino H, Takagi M, Takeuchi I, Akutsu T, Takagi Y, Ebihara S. Recanalization of intracranial carotid occlusion detected by duplex carotid sonography. Stroke 1989;20:680–6.

Jahan R, Duckwiler GR, Kidwell CS, Sayre JW, Gobin YP, Villablanca JP, Saver J, Starkman S, Martin N, Vinuela F. Intraarterial thrombolysis for treatment of acute stroke: experience in 26 patients with long-term follow-up. Am J Neuroradiol 1999;20:1291–9.

Jansen O, von Kummer R, Forsting M, Hacke W, Sartor K. Thrombolytic therapy in acute occlusion of the intracranial internal carotid artery bifurcation. Am J Neuroradiol 1995;16:1977–86.

Kimura K, Yonemura K, Terasaki T, Hashimoto Y, Uchino M. Duplex carotid sonography in distinguishing acute unilateral atherothrombotic from cardioembolic carotid artery occlusion. Am J Neuroradiol 1997;18:1447–52.

Koga M, Kimura K, Minematsu K, Yamaguchi T. Diagnosis of internal carotid artery stenosis greater than 70% with power doppler duplex sonography. Am J Neuroradiol 2001;22:413–7.

Krieger DW, Demchuk AM, Kasner SE, Jauss M, Hantson L. Early clinical and radiographical predictors of fatal brain swelling in ischemic stroke. Stroke 1999;30:287–92.

Leys D, Pruvo JP, Godefroy O, Rondepierre P, Leclerc X. Prevalence and significance of hyperdense middle cerebral artery in acute stroke. Stroke 1992;23:317–24.

Manelfe C, Larrue V, von Kummer R, Bozzao L, Ringleb P, Bastianello S, Iweins F, Lesaffre E. Association of hyperdense middle cerebral artery sign with clinical outcome in patients treated with tissue plasminogen activator. Stroke 1999;30:769–72.

Marks MP, Holmgren EB, Fox AJ, Patel S, von Kummer R, Froehlich J. Evaluation of early computed tomographic findings in acute ischemic stroke. Stroke 1999;30:389–92.

Moulin T, Cattin F, Crepin-Leblond T, Tatu L, Chavot D, Piotin M, Viel JF, Rumbach L, Bonneville JF. Early CT signs in acute middle cerebral artery infarction: predictive value for subsequent infarct localization and outcome. Neurology 1996;47:366–75.

Muir KW, Weir CJ, Murray GD, Povey C, Lees KR. Comparison of neurological scales and scoring systems for acute stroke prognosis. Stroke 1996;27:1817–20.

Oxbury JM, Greenhall RC, Grainger KM. Predicting the outcome of stroke: acute stage after cerebral infarction. Br Med J 1975;3:125–7.

The National Institute of Neurological Disorders and Stroke rt-PA Stroke Study Group. Tissue plasminogen activator for acute ischemic stroke. New Engl J Med 1995;333:1581–7.

Tomsick TA, Brott TG, Chambers AA, Fox AJ, Gaskill MF, Lukin RR, Pleatman CW, Wiot JG, Bourekas E. Hyperdense middle cerebral artery sign on CT: efficacy in detecting middle cerebral artery thrombosis. Am J Neuroradiol 1990;11:473–7.

Tomura N, Uemura K, Inugami A, Fujita H, Higano S, Shishido F. Early CT finding in cerebral infarction: obscuration of the lentiform nucleus. Radiology 1988;168:463–7.

Truwit CL, Barkovich AJ, Gean-Marton A, Hibri N, Norman D. Loss of the insular ribbon: another early CT sign of acute middle cerebral artery infarction. Radiology 1990;176:801–6.

Urbach H, Ries F, Ostertun B, Solymosi L. Local intra-arterial fibrinolysis in thromboembolic 'T' occlusions of the internal carotid artery. Neuroradiology 1997;39:105–10.

van Swieten JC, Koudstaal PJ, Visser MC, Schouten HJ, van Gijn J. Interobserver agreement for the assessment of handicap in stroke patients. Stroke 1988;19:604–7.

von Kummer R, Meyding-Lamade U, Forsting M, Rosin L, Rieke K, Hacke W, Sartor K. Sensitivity and prognostic value of early CT in occlusion of the middle cerebral artery trunk. Am J Neuroradiol 1994;15:9–15.

Yasaka M, Omae T, Tsuchiya T, Yamaguchi T. Ultrasonic evaluation of site of carotid axis occlusion in patients with acute cardioembolic stroke. Stroke 1992;23:420–2.

Journal of Cerebral Blood Flow & Metabolism
22:835–842 © 2002 The International Society for Cerebral Blood Flow and Metabolism
Published by Lippincott Williams & Wilkins, Inc., Philadelphia

Unique Profile of Spreading Depression in a Primate Model

*Chiaki Yokota, †Yuji Kuge, ‡Yasuhiro Hasegawa, ‡Masafumi Tagaya, §Takeo Abumiya, ‖Norimasa Ejima, ¶Nagara Tamaki, ‡Takenori Yamaguchi, and ‡Kazuo Minematsu

*Departments of *Pathogenesis and §Epidemiology, Research Institute, and ‡Cerebrovascular Division, Department of Medicine, National Cardiovascular Center, Osaka; †Department of Tracer Kinetics, Graduate School of Medicine, Hokkaido University, Sapporo; ‖Institute for Biofunctional Research Co., Osaka; and ¶Department of Nuclear Medicine, Graduate School of Medicine, Hokkaido University, Sapporo, Japan*

Summary: Spreading depression (SD) is considered to play a role in pathologic conditions of humans such as in the evolution of ischemic brain injury and migraine aura. Because many studies have demonstrated spreading hypoperfusion in patients with migraine and persistent hypoperfusion in nonprimate animal models of SD, these changes in cerebral blood flow (CBF) were regarded as an epiphenomenon of SD. However, there is no direct evidence of the occurrence of SD in primates. The authors attempted to elicit SD by applying 3.3 mol/L potassium chloride to the cerebral cortex of nine male cynomolgus monkeys. The CBF was monitored by positron emission tomography in five animals. Propagated direct-current shifts were found by the two neighboring microelectrodes only in one animal. The direct-current wave propagated at a speed of 4 mm/min and its amplitude was 20 mV, being consistent with the SD findings. Except in one animal with 6 SD episodes, SD waves were recorded infrequently at the rostral site (none in three animals, once in three, and twice in two). Focal hyperemia accompanied SD. Neither spreading hypoperfusion nor persistent hypoperfusion was found. These unique features of SD in primates raise a doubt as to whether the role of SD in nonprimate animals is the same as that in stroke and migraine in humans. **Key Words:** Spreading depression—Primate—PET.

Cortical spreading depression (SD), which was first reported by Leao (1944), is characterized by reversible depression of cortical electrical activity in the brain that spreads like a wave at a speed of 2 to 5 mm per minute. Spreading depression can be induced by a variety of experimental stimuli such as electrical, chemical, and mechanical stimuli. Spreading depression has been observed in rats (Lauritzen et al., 1982; Iijima et al., 1992; Gardner-Medwin et al., 1994; Hasegawa et al., 1995; Takano et al., 1996), cats (Piper et al., 1991; Saito et al., 1995; Kuge et al., 2000), and a patient with severe head injury (Mayevsky et al., 1996).

There is strong experimental evidence that repetitive pathologic SDs in the periinfarct border zone contribute to the evolution of infarcts in rat and cat models (Gill et al., 1992; Iijima et al., 1992; Chen et al., 1993; Nedergaard and Hansen, 1993; Back et al., 1994; Hossmann, 1994; Takano et al., 1996; Ohta et al., 2001). Because ischemia-related SDs are considered to exacerbate the preexisting energy depletion in the periinfarct zone (Hossmann, 1994; Takano et al., 1996), they are regarded as a target of pharmacologic intervention. Although most neuroprotective agents that block the occurrence of SDs in rodents (Gill et al., 1992; Iijima et al., 1992; Chen et al., 1993) work well during brain ischemia in such small animals (del-Zoppo et al., 1997), the majority of potential neuroprotective therapies modifying ischemic cell death cascades did not have beneficial effects in patients who had had a stroke.

Transient cortical hyperemia followed by persistent hypoperfusion was reported to be an epiphenomenon of SD in rat- and cat-SD models (Lauritzen et al., 1982; Piper et al., 1991; Kuge et al., 2000). Spreading depression has been speculated to underlie migraine visual aura based on indirect evidence from human neuroimaging studies (Olesen et al., 1981; Lauritzen et al., 1983; Lauritzen and Olesen, 1984; Woods et al., 1994; Hadjikhani et al., 2001). Because spreading hypoperfusion was

Received January 7, 2002; final version received March 11, 2002; accepted March 11, 2002.

Supported in part by the Special Coordination Funds for Promoting Science and Technology (Strategic Promotion System for Brain Science) from the Ministry of Education, Culture, Sports, Science and Technology of Japan, and a Grant-in-Aid for Scientific Research from the Japan Society for the Promotion of Science.

Address correspondence and reprint requests to Chiaki Yokota, Cerebrovascular Laboratory, National Cardiovascular Center Research Institute, 5-7-1 Fujishirodai, Suita, Osaka, 565-8565, Japan; e-mail: cyokota@ri.ncvc.go.jp

demonstrated during a migraine attack in these previous studies (Olesen et al., 1981; Lauritzen et al., 1983; Lauritzen and Olesen, 1984; Woods et al., 1994; Hadjikhani et al., 2001), it is regarded as an attendant change in cerebral blood flow (CBF) on SD in patients with migraine attacks. However, the hypothesis that aura underlain by SD phenomenon might be the trigger for migraine, particularly being pivotal to pain, was indicated to be implausible from the clinical point of view (Goadsby, 2001). Recently, Ebersberger et al. (2001) did not see any proof of neurogenic inflammation in migraine headache. Furthermore, there are no reports providing direct evidence that SD, characterized by the reversible depression of cortical electrical activity, can be elicited in primates, although a few studies suggested the occurrence of SD by measuring the changes in cortical fluorescence (Strong et al., 2000), the kinetics of resolution of extracellular potassium activity (Branston et al., 1977), and recording the slow potential of lissencephalic cortex in squirrel monkey (Robert, 1970).

The participation of SD in various neuronal disorders in humans has been a matter of speculation. In the current study, we attempted to clarify whether SD can be evoked in primates. In addition, we examined the attendant changes in the CBF during the provocation of SD using positron emission tomography (PET).

MATERIALS AND METHODS

Animal preparation

All procedures in this study were approved by our Institutional Animal Research Committee and were performed in accordance with the standards published by the National Research Council (Guide for the Care and Use of Laboratory Animals). In compliance with these standards, every effort was made to ensure that the animals were free from pain or discomfort. The principal investigator and primate handling staff were present for all procedures. The monkeys were individually in cages larger than 63 cm (width) × 76 cm (height) × 76 cm (depth) and maintained on a 12-hour light/dark cycle (lights on at 8:00 a.m.). All animals were neurologically normal and had no evidence of infections or inflammation immediately before the experiments.

Nine adult, male cynomolgus monkeys (nos. 1 through 9) were anesthetized with pentobarbital (50 mg/kg, intraperitoneally), followed by tracheal intubation. Then, the anesthetic state was maintained with N_2O/O_2 (70%:30%) gas mixture inhalation under artificial ventilation. Any other anesthetic agents were not added during the experimental period. The rectal temperature was monitored continuously with a rectal probe and maintained at approximately 36°C with a heating pad. An arterial catheter was used for continuous monitoring of heart rate and arterial pressure.

Electrophysiologic measurement

The anesthetized animal was mounted on a custom-made stereotaxic instrument in a prone position, and the head was restrained using teeth- and ear-bars. After the frontoparietal cranium was exposed by a midsagittal incision, three to four small burr holes were made in the left parietal skull bone and the dura was carefully excised; one burr hole was used for KCl application and two to three were used for direct current (DC) potential recordings. Of these, two burr holes were made rostral to the hole for KCl application in all animals, for recording the DC potential through microelectrodes inserted into the cortical surface. Another hole for recording the DC potential was made caudal to the hole for KCl application, in two animals (nos. 4 and 5). These burr holes were made along a line at 7-mm intervals. We also recorded the DC shift in the right parietal skull in one monkey (no. 4), although it has been reported that SD waves do not spread to the contralateral hemisphere (Marshall, 1959; Hasegawa et al., 1995).

The DC potential was monitored with an amplifier (Iso-DAM8; World Precision Instruments, Sarasota, FL, U.S.A.) by microelectrodes that had been inserted into the cortex to a depth of 1 mm. Physiologic saline followed by KCl solution was applied to the cortex through one of the burr holes. The KCl solution was applied up to 3 times at intervals of 10 minutes until a SD was elicited by the KCl. The concentration of KCl of 3.3 mol/L was chosen, because lower concentrations such as 0.15 mol/L and 1 mol/L did not induce SD in our preliminary study with monkeys (data not shown).

At 120 minutes after KCl application, the brain tissues of animals that did not undergo the PET study described in the next section were perfused with cold saline and the animals were killed by exsanguination under pentobarbital anesthesia. The brain was quickly removed, and several samples were dissected out and stored at −80°C for future analyses. A sagittal slice through the insertion sites of the two microelectrodes was obtained from one monkey (no. 7) to measure the length of the cortical surface between the two microelectrodes.

Positron emission tomography study

Positron emission tomography was performed with a multislice PET scanner (ECAT EXACT HR/47; Siemens/CTI, Knoxville, TN, U.S.A.) (Wienhard et al., 1994), which provides 47 tomographic images at 3.1-mm intervals per frame. The spatial resolution at the center of the field of view was 3.7 mm in-plane at full width at half maximum and 4.1 mm axially.

Five of the nine animals (nos. 1 to 5) underwent the PET study simultaneously with the recording of SD waves. The animal was placed in the field of view in the prone position and the head was restrained by teeth- and ear-bars. In the PET experiments, the brain position was standardized with the aid of laser beams. This enabled us to correlate PET images with the outer orbital point and the meatus auditorius. Positron emission tomography images were then correlated with the locations of stimulation and DC potential measurement. Blood gas and blood sugar analyses were performed in blood samples obtained from the femoral artery before and 120 minutes after the KCl application. The CBF was measured by PET with an intravenous bolus injection of ^{15}O-labeled water. Dynamic PET scanning (0 to 2 minutes) was initiated at the time of the ^{15}O-H_2O injection. A baseline CBF measurement (Pre) was made before the topical application of 3.3 mol/L of KCl solution in all animals. In three animals (nos. 1 to 3), the CBF was also measured before the administration of physiologic saline to confirm that the mean hemispheric CBF before administration of KCl solution was in the same range as that before the administration of physiologic saline. In the animals with SD occurrence, the CBF was measured within 10 minutes after the first SD was elicited (CBF_1), followed by 3 to 5 PET scans at intervals of approximately 10 to 20 minutes. If a SD was not elicited, the CBF_1 was measured 10 minutes after the third KCl application, followed by 3 PET scans that were obtained in the same manner as in the other animals that had SDs.

After the PET study was completed, the brain tissues were perfused with cold saline and the animals were killed in the same manner as those that did not undergo the PET study. Several samples obtained from the brain were stored at −80°C for future study.

Data analysis

The PET images were reconstructed according to a standard filtered back-projection procedure using a Hanning filter. Each activity image was globally normalized by relative ratio to regional counts of the cerebellar cortex ipsilateral to the site of KCl application. Time courses of CBF changes for every frame in either transaxial or coronal images were ascertained by the visual inspection by two of the authors (Y.K. and N.E.), whether there were any areas of persistent hypoperfusion as compared with the contralateral hemisphere, and also spreading hypoperfusion was observed following primary hyperperfusion after SD. In addition, a total of 14 circular regions of interest were positioned in each hemisphere symmetrically on three transaxial brain slices as shown in Fig. 1. Considering the spatial resolution of the PET apparatus in the present study, the diameter of regions of interest (ROIs) was 8 mm (0.5 cm^2 in area), twice as much as the value of full width at half maximum. Because of various problems as pointed by Heiss et al. (1994), that is, with repeated withdrawal of blood during prolonged experimental periods, partial volume effects, and excluding the effects associated with variations in levels of anesthesia, we used the asymmetry index, which was defined as the ratio of the value of regional CBF in the ROI in the hemisphere ipsilateral to the site of KCl application to that in the contralateral homologous ROI.

Data are expressed as the mean ± SD, unless otherwise noted. The significance of differences in the sequential change of each physiologic parameter was assessed using repeated-measures one-way analysis of variance and Fischer's PLSD *post hoc* test. A two-tailed P value less than 0.05 was considered to be significant.

RESULTS

Electrophysiologic study

During the experimental period, physiologic parameters of the monkeys including body temperature, heart rate, mean arterial pressure, blood sugar, and blood gas levels did not change significantly (Table 1).

The number and location of DC shifts elicited by the KCl in each monkey are listed in Table 2. Shifts of DC potential were recorded through the microelectrode just rostral to the site of chemical stimulation in only five of the nine monkeys: a single episode was recorded in three monkeys (nos. 3, 6, and 7), two episodes in one monkey (no. 2), and six episodes in one monkey (no. 9). Of the two animals with the caudal hole, animal 5 had eight episodes in the site caudal to the site of chemical stimulation, but no DC shift at the rostral sites. The other animal (no. 4) had two DC shifts, each of which was rostrally adjacent to the site of chemical stimulation, and six episodes at the caudal site, but no episodes at the contralateral site.

A propagated DC shift was found on the recordings of DC potentials in two neighboring microelectrodes 7 mm apart in only one animal (no. 7). In this monkey, the length of the cortical convolution between the 2 microelectrodes was 48 mm. The DC shift spread between the two microelectrodes in 12 minutes (Fig. 2A), resulting in a propagation speed of 4 mm per minute. The amplitude was 20 mV. These values are consistent with the SD findings reported in previous studies (Leao, 1944; Marshall, 1959). The representative image of repetitive SD waves in animal 9 is shown in Fig. 2B. Propagation of

FIG. 1. Examples of regions of interest (ROIs; each ROI had an area of 0.5 cm^2) placed on three transaxial images. The slices are approximately 2.5 cm, 3.2 cm, and 4.2 cm, respectively, from the top of the precentral gyrus in the field of view. Fourteen circular ROIs were placed on the cerebral cortex ipsilateral to the site of KCl application, and 14 additional ROIs were placed symmetrically in the contralateral hemisphere. The ROI rostrally adjacent to the site of KCl application is indicated with a blue circle; the one caudally adjacent to the KCl application site is shown in pink; and the KCl application site is indicated with a yellow circle.

TABLE 1. *Serial changes in physiologic variables*

Parameter		Time after KCl application (min) 0*	20	60	120	P†
Body temperature (°C)	Mean	36.1	36.0	36.1	36.3	NS
	SD	1.6	1.6	1.9	1.9	
Heart rate (beat/min)	Mean	156	149	149	149	NS
	SD	26	28	30	32	
Mean arterial pressure (mm Hg)	Mean	91	92	92	91	NS
	SD	21	21	23	21	
Plasma glucose concentration (mg/100 mL)	Mean	83.8	—	—	85.1	NS
	SD	25.1	—	—	11.6	
pH	Mean	7.5	—	—	7.5	NS
	SD	0.05	—	—	0.04	
Po_2 (mm Hg)	Mean	177.8	—	—	174.3	NS
	SD	19.7	—	—	22.5	
Pco_2 (mm Hg)	Mean	35.7	—	—	34.3	NS
	SD	3.1	—	—	4.8	

The body temperature, heart rate, and mean aterial pressure were measured in all 9 animals. The blood glucose and blood gas levels at 0 minutes and 120 minutes after potassium chloride (KCl) application were measured in the 5 animals that underwent the PET study.

SD, standard deviation; NS, not significant ($P > 0.05$); —, not measured.

* Values before KCl application; †repeated measures one-way ANOVA.

SD waves was not detected in the rostral hole distant from the site of KCl application.

Positron emission tomography study

By the visual inspection of all images of the PET study including transaxial and coronal ones, there were neither areas of persistent hypoperfusion nor spreading hypoperfusion following primary hyperperfusion after SD in any animals. Representative, multislice PET images of animal 4 in which SD was recorded twice at the rostral site and six times at the caudal site are shown in Fig. 3. Six episodes at the caudal site and one episode at the rostral site were detected immediately after KCl application, and another rostral episode occurred between the measurement of CBF_1 and CBF_2. The PET images obtained after the occurrence of SD demonstrated transient focal hyperemia in the occipital cortex caudally adjacent to the site of KCl application. In the hemisphere contralateral to the site of KCl application, there were no remarkable changes in regional CBF throughout the PET study in any of the animals.

Figure 4 shows the change in the asymmetry index of CBF in the 14 ROIs over time before and after the SDs in each of the 5 animals in the PET study. Focal increases in regional CBF were observed in accordance with the occurrence of SD in each animal. During the experiment, the asymmetry index increased by a maximum of 1.2 to 1.7 times in various ROIs in the five animals. In animal 1, in which no SD episodes had been detected at the rostral sites, focal hyperemia was observed after the chemical stimulation. However, none of the animals had persistent hypoperfusion in any ROIs.

TABLE 2. *Number of direct-current shifts detected by the microelectrodes at each site*

Animal no.	Rostral site* (close/distal)	Caudal site	Contralateral site	PET study
1	0/0	—	—	Yes
2	2/0	—	—	Yes
3	1/0	—	—	Yes
4	2/0	6	0	Yes
5	0/0	8	—	Yes
6	1/0	—	—	No
7	1/1	—	—	No
8	0/0	—	—	No
9	6/0	—	—	No

—, not measured.

* Two burr holes were made rostral to the site of chemical stimulation. One direct-current (DC) shift in animal 7 was detected at the rostral site distant from the site of potassium chloride (KCl) stimulation. All other DC shifts were detected at the site just rostral to the site of KCl stimulation.

DISCUSSION

This is the first report that provides direct evidence that SD can be evoked in primates. It is known that SD waves propagate predominantly toward the caudal direction (Leao, 1944), and the present results were consistent with this. However, the measurements of SD at caudal positions were performed only in two of nine monkeys in the present study. Thus, the question as to whether SD preferentially propagates in a posterior direction remains obscure. Spreading depression waves can readily be elicited in the lissencephalic cortices (Saito et al., 1995).

In a rat model, SD waves propagated throughout a hemisphere (Hasegawa et al., 1995). In the present study, however, SD waves were infrequently detected at the rostral site close to the source of stimulation. Only a single SD was detected at the site distant from the stimulation. Because measurements of SD waves were examined by a limited number of electrodes in the present

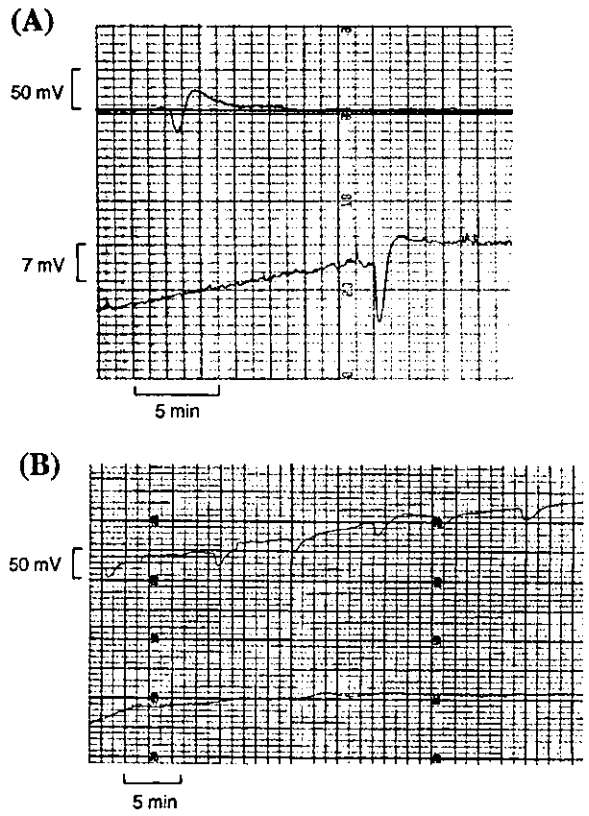

FIG. 2. Characteristics of spreading depression waves. **(A)** Propagation of a spreading depression (SD) wave. Recordings of the direct current (DC) potential obtained from the rostral holes close to (red line) and distant from (blue line) the site of KCl application in animal 7 are shown. A gain of amplitude is different between red and blue lines: red line: ×10, blue line: 10^2. Although the straight distance between the two microelectrodes was 7 mm, the length of the cortical convolution between them was 48 mm. Because the time lag between the waves was 12 minutes, the propagation velocity of the wave on the cortical convolution was 4.0 mm/min. **(B)** Repetitive episodes of spreading depression waves. The red line shows the DC potential obtained from the rostral hole close to and the blue line goes distant from the site of KCl application in animal 9. Propagation of SD waves was not observed in this animal.

study, it may be difficult to confirm that no SD waves were detected. The detection of SD was also reported to depend on several factors, including the depths of electrode insertion into cortical tissue (Richter and Lehmenkuhler, 1993). However, we reported previously that more than 13 SD episodes could be evoked in the rostral direction in cats under the same experimental conditions as the present study (Kuge et al., 2000). SD waves can hardly be elicited, and propagate within a narrow range in primates. Differences in the cytoarchitecture among species, which are considered to reflect differences in the number and length of dendritic and axonal ramifications (Rockel et al., 1980), would influence the propagation of SD.

The CBF pattern obtained in the present study differs from those obtained in rat- and cat-SD models (Lauritzen et al., 1982; Piper et al., 1991; Kuge et al., 2000). In this study, we could not observe the prolonged hypoperfusion after the focal hyperemia. Although the size of ROIs was determined considering the spatial resolution of the PET apparatus, the possibility cannot be completely excluded that the PET would be insufficiently accurate in measuring CBF changes because of calculation of the limited number of ROIs, and the possibility of the mismatch between the ROI and the mirror region in the contralateral hemisphere. Therefore, we also ascertained by visual inspection of all PET images that there were no areas of persistent hypoperfusion as compared with the contralateral hemisphere, and also no spreading hypoperfusion was observed following focal hyperemia after SD. KCl application has been widely used because it is one of the most reliable methods of evoking SD (Marshall, 1959; Hasegawa et al., 1995; Saito et al., 1995; Takano et al., 1996; Kuge et al., 2000). An increased extracellular potassium concentration *per se* may increase blood flow. However, the pattern of the serial change in CBF after KCl application varied depending on the SD profile in the five animals that underwent the PET study. Although

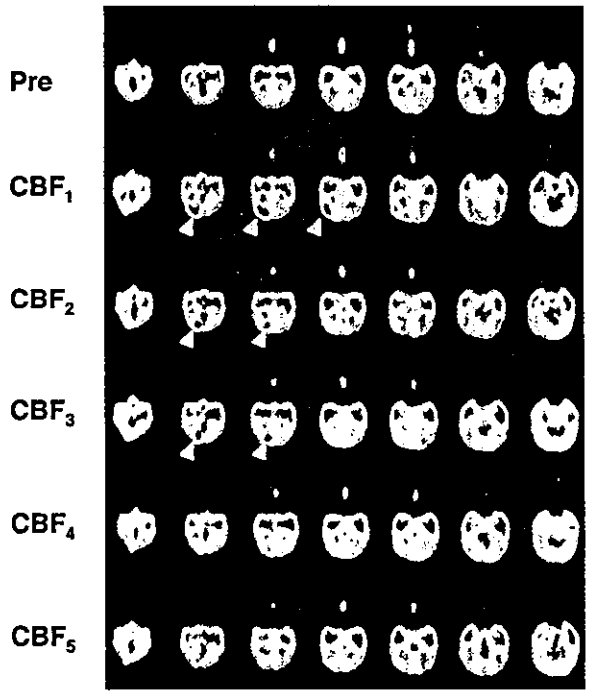

FIG. 3. Representative positron emission tomography (PET) images showing the time course of cerebral blood flow (CBF) changes. The time course of the change in CBF in transaxial slices of 3.1-mm width before (Pre) and at various time points after KCl application in animal 4 is shown. The first PET scan after KCl application (CBF_1) was taken within 10 minutes after the first spreading depression was detected. Thereafter, 4 PET scans at intervals of 10 to 20 minutes (CBF_2, CBF_3, CBF_4, CBF_5) were obtained. The PET scans in a column represent those taken at the same transaxial slice. The multislice PET images showed transient focal hyperemia (arrowhead) in the occipital cortex caudally adjacent to the site of KCl application.

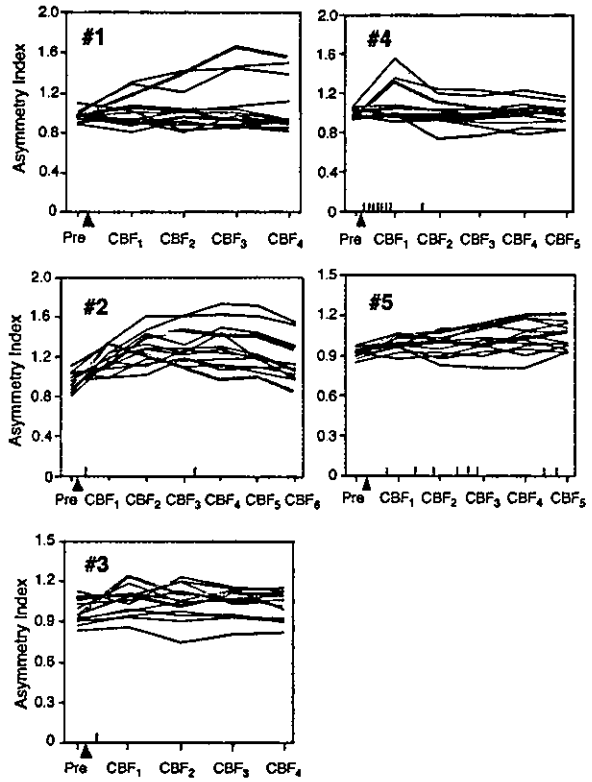

FIG. 4. Course of the asymmetry index of cerebral blood flow (CBF) in the 14 regions of interest (ROIs) in each of the 5 animals that underwent the positron emission tomography study. The blue, pink, and yellow lines show the changes in the asymmetry index in the ROIs indicated by blue, pink, and yellow, respectively, in Fig. 1. The arrowhead indicates the time point of KCl application for eliciting spreading depressions (SDs). The time points at which SD was detected are indicated with vertical short lines above the *x* axis: a blue line indicates SD to the rostral direction, and a pink line indicates SD to the caudal direction. Focal increases in regional CBF were observed in accordance with the occurrence of SD in each animal. However, persistent hypoperfusion was not seen in any of the animals.

animal 1 did not show SD to the rostral direction, the pattern of the serial CBF change in this animal was similar to that in animal 5 that had eight SD episodes to the caudal direction but no episodes to the rostral direction. The dynamics of the CBF after chemical stimulation appear to be determined by the timing as well as the number of SD episodes.

Duckrow (1991) advocated a hypothesis using a rat model that hyperemia after SD would be observed only in anesthetized animals, whereas long-lasting hypoperfusion would occur after SD in both the conscious and anesthetized conditions. We previously demonstrated that a long-lasting CBF reduction followed a transient increase in CBF after a single SD in the cortex ipsilateral to the site of KCl application in cats (Kuge et al., 2000), which is consistent with a rat-SD model (Lauritzen et al., 1982). Flow-metabolism uncoupling with persistent hypoperfusion in the cortex of cats with SD indicated that cerebrovascular reactivity was impaired in association with SD (Kuge et al., 2000). In this study, persistent hypoperfusion was not seen in any ROI in the five animals. Wahl et al. (1987) demonstrated that the vascular responses to SD differed between cats and rats. Based on our study, the vascular responses to SD in primates may also differ from those in cats.

The changes in CBF during an SD phenomenon in primates also differed from those in patients with migraine (Olesen et al., 1981; Lauritzen et al., 1983; Lauritzen and Olesen, 1984; Woods et al., 1994; Hadjikhani et al., 2001), although the scanning procedures and data analysis of PET were the same as those of the previous report (Woods et al., 1994). Because a pain stimulus results in a reduction in global CBF in humans (Coghill et al., 1998), the migraine headache itself may influence the dynamics of CBF in patients with a migraine attack. It was also indicated that SD may not be associated with migraine headache (Ebersberger et al., 2001). Furthermore, SD in the human brain, if present, would propagate much more slowly than observed in a previous migraine study (Woods et al., 1994), because SD waves propagate on the cortical convolution.

One should be cautious about projecting our results to the ischemic brain of primates and questioning the role of SDs in the evolution of brain infarction. Spreading depression is a fully reversible process in the normal brain and does not cause neuronal damage (Nedergaard and Hansen, 1988). However, in moderately ischemic brain as is present in the ischemic penumbra, SD waves, namely, periinfarct depolarizations, may be associated with episodic energy failure in the acute ischemic penumbra in primates, as demonstrated in rats (Back et al., 1996). We have reported recently that a CBF and cerebral metabolic rate of glucose uncoupling was observed in the parietal cortex and several regions surrounding the ischemic core in a primate model of thromboembolic stroke (Kuge et al., 2001). Although the mechanisms underlying the elevated glucose metabolism and the process of uncoupling of flow and metabolism remained to be clarified, anaerobic glycolysis and SD are proposed as factors contributing to elevated glucose metabolism in early phases of ischemia (Ginsberg et al., 1977; Shinohara et al., 1979; Tanaka et al., 1985; Hasegawa et al., 1990; Back et al., 1995; Kuge et al., 2000). The contribution of SD to pathophysiology of ischemic stroke cannot be resolved by the findings obtained from the present study. However, the poor migration of SDs and rare evidence of migrating SD waves in primates may account for the negative result in patients with stroke (Back et al., 2000).

The present study suggests that one must be careful when applying the experimental results of SD obtained from nonprimate animals to the pathogenesis of brain diseases in humans. The dynamics of SDs may vary among species because of differences in convolutional

and cytoarchitectural structure, and the vascular responses to SDs. First, SD occurred less frequently in our primate model than in nonprimate models. Its propagation was limited to areas near the site of stimulation in the cynomolgus monkeys, although it propagated to the entire hemisphere in rats. Second, immediately after the first SD was elicited, focal cortical hyperemia was detected, but it was not followed by spreading hypoperfusion or persistent hypoperfusion in the hemisphere ipsilateral to the site of chemical stimulation. These unique features of SD in this primate demand reappraisal of the hypothesis that SD contributes to the pathogenesis of human brain diseases.

REFERENCES

Back T, Kohno K, Hossmann KA (1994) Cortical negative DC deflections following middle cerebral artery occlusion and KCl-induced spreading depression: effect on blood flow, tissue oxygenation, and electroencephalogram. *J Cereb Blood Flow Metab* 14:12–19

Back T, Zhao W, Ginsberg MD (1995) Three-dimensional image analysis of brain glucose metabolism-blood flow uncoupling and its electrophysiological correlates in the acute ischemic penumbra following middle cerebral artery occlusion. *J Cereb Blood Flow Metab* 15:566–577

Back T, Ginsberg MD, Dietrich WD, Watson BD (1996) Induction of spreading depression in the ischemic hemisphere following experimental middle cerebral artery occlusion: effect on infarct morphology. *J Cereb Blood Flow Metab* 16:202–213

Back T, Hirsch JG, Szabo K, Gass A (2000) Failure to demonstrate peri-infarct depolarizations by repetitive MR diffusion imaging in acute human stroke. *Stroke* 31:2901–2906

Branston NM, Strong AJ, Symon L (1977) Extracellular potassium activity, evoked potential and tissue blood flow: relationship during progressive ischemia of baboon cerebral cortex. *J Neurol Sci* 32:305–321

Chen Q, Chopp M, Bodzin G, Chen H (1993) Temperature modulation of cerebral depolarization during focal cerebral ischemia in rats: correlation with ischemic injury. *J Cereb Blood Flow Metab* 13:389–394

Coghill RC, Sang CN, Berman KF, Bennett GJ, Iadarola MJ (1998) Global cerebral blood flow decreases during pain. *J Cereb Blood Flow Metab* 18:141–147

del-Zoppo GJ, Wagner S, Tagaya M (1997) Trends and future developments in the pharmacological treatment of acute ischemic stroke. *Drugs* 54:9–38

Duckrow RB (1991) Regional cerebral blood flow during spreading cortical depression in conscious rats. *J Cereb Blood Flow Metab* 11:150–154

Ebersberger A, Schaible HG, Averbeck B, Richter F (2001) Is there a correlation between spreading depression, neurogenic inflammation, and nociception that might cause migraine headache? *Ann Neurol* 49:7–13

Gardner-Medwin AR, vanBruggen N, Williams SR, Ahier RG (1994) Magnetic resonance imaging of propagating waves of spreading depression in the anesthetised rat. *J Cereb Blood Flow Metab* 14:7–11

Gill R, Andine P, Hillered L, Persson L, Hagberg H (1992) The effect of MK-801 on cortical spreading depression in the penumbral zone following focal ischemia in the rat. *J Cereb Blood Flow Metab* 12:371–379

Ginsberg MD, Reivich M, Giandomenico A, Greenberg JH (1977) Local glucose utilization in acute focal cerebral ischemia: local dysmetabolism and diaschisis. *Neurology* 27:1042–1048

Goadsby PJ (2001) Migraine, aura, and cortical spreading depression: why are we still talking about it? *Ann Neurol* 49:4–6

Hadjikhani N, del-Rio MS, Wu O, Schwartz D, Bakker D, Fischl B, Kwong KK, Cutrer FM, Rosen BR, Tootell RBH, Sorensen AG, Moskowitz MA (2001) Mechanisms of migraine aura revealed by functional MRI in human visual cortex. *Proc Natl Acad Sci U S A* 95:811–817

Hasegawa Y, Choki J, Yamaguchi T (1990) Cerebral blood flow, glucose utilization, and electrocorticograms following common carotid artery occlusion in gerbils. *Stroke* 21:112–118

Hasegawa Y, Latour LL, Formato JE, Sotak CH, Fisher M (1995) Spreading waves of a reduced diffusion coefficient of water in normal and ischemic rat brain. *J Cereb Blood Flow Metab* 15:179–187

Heiss W-D, Graf R, Wienhard K, Saito LR, Fujita T, Rosner G, Wagner R (1994) Dynamic penumbra demonstrated by sequential multitracer PET after middle cerebral artery occlusion in cats. *J Cereb Blood Flow Metab* 14:892–902

Hossmann KA (1994) Viability thresholds and the penumbra of focal ischemia. *Ann Neurol* 36:557–565

Iijima T, Mies G, Hossmann KA (1992) Repeated negative DC deflections in rat cortex following middle cerebral artery occlusion are abolished by MK-801: effect on volume of ischemic injury. *J Cereb Blood Flow Metab* 12:727–733

Kuge Y, Hasegawa Y, Yokota C, Minematsu K, Hashimoto N, Miyake Y, Yamaguchi T (2000) Effects of single and repetitive spreading depression on cerebral blood flow and glucose metabolism in cats: a PET study. *J Neurol Sci* 176:114–123

Kuge Y, Yokota C, Tagaya M, Hasegawa Y, Nishimura A, Kito G, Tamaki N, Hashimoto N, Yamaguchi T, Minematsu K (2001) Serial changes in cerebral blood flow and flow-metabolism uncoupling in primates with acute thromboembolic stroke. *J Cereb Blood Flow Metab* 21:202–210

Lauritzen M, Jorgensen MB, Diemer NH, Gjedde A, Hansen AJ (1982) Persistent oligemia of rat cerebral cortex in the wake of spreading depression. *Ann Neurol* 12:469–474

Lauritzen M, Olesen J (1984) Regional cerebral blood flow during migraine attacks by Xenon-133 inhalation and emission tomography. *Brain* 107:447–461

Lauritzen M, Olsen TS, Lassen NA, Paulson OB (1983) Changes in regional cerebral blood flow during the course of classic migraine attacks. *Ann Neurol* 13:633–641

Leao AAP (1944) Spreading depression of activity in the cerebral cortex. *J Neurophysiol* 7:359–390

Marshall WH (1959) Spreading cortical depression of Leao. *Physiol Rev* 39:239–279

Mayevsky A, Doron A, Manor T, Meilin S, Zarchin N, Ouaknine GE (1996) Cortical spreading depression recorded from the human brain using a multiparametric monitoring system. *Brain Res* 740:268–274

Nedergaard M, Hansen AJ (1988) Spreading depression is not associated with neuronal injury in the normal brain. *Brain Res* 449:395–398

Nedergaard M, Hansen AJ (1993) Characterization of cortical depolarizations evoked in focal cerebral ischemia. *J Cereb Blood Flow Metab* 13:568–574

Ohta K, Graf R, Rosner G, Heiss W-D (2001) Calcium ion transients in peri-infarct depolarizations may deteriorate ion homeostasis and expand infarction in focal cerebral ischemia in cats. *Stroke* 32:535–543

Olesen J, Larsen B, Lauritzen M (1981) Focal hyperemia followed by spreading oligemia and impaired activation of rCBF in classic migraine. *Ann Neurol* 9:344–352

Piper RD, Lambert GA, Duckworth JW (1991) Cortical blood flow changes during spreading depression in cats. *Am J Physiol* 261:H96–H102

Richter F, Lehmenkuhler A (1993) Spreading depression can be restricted to distinct depths of the rat cerebral cortex. *Neurosci Lett* 152:65–68

Robert CS (1970) Spreading depression in squirrel monkey lissencephalic cortex. *Physiol Behav* 1970:239–241

Rockel AJ, Hiorns RW, Powell TPS (1980) The basic uniformity in structure of the neocortex. *Brain* 103:221–244

Saito R, Graf R, Hubel K, Taguchi J, Rosner G, Fujita T, Heiss W-D (1995) Halothane, but not a-chloralose, blocks potassium-evoked cortical spreading depression in cats. *Brain Res* 699:109–115

Shinohara M, Dollinger B, Brown G, Rapoport S, Sokoloff L (1979)

Cerebral glucose utilization: local changes during and after recovery from spreading cortical depression. *Science* 203:188–190

Strong AJ, Smith SE, Whittington DJ, Meldrum BS, Parsons AA, Krupinski J, Hunter AJ, Patel S (2000) Factors influencing the frequency of fluorescence transients as markers of peri-infarct depolarizations in focal cerebral ischemia. *Stroke* 31:214–222

Takano K, Latour LL, Formato JE, Carano RAD, Helmer KG, Hasegawa Y, Sotak CH, Fisher M (1996) The role of spreading depression in focal ischemia evaluated by diffusion mapping. *Ann Neurol* 39:308–318

Tanaka K, Greenberg JH, Gonatas NK, Reivich M (1985) Regional flow-metabolism coupling following middle cerebral artery occlusion in cats. *J Cereb Blood Flow Metab* 5:241–252

Wahl M, Lauritzen M, Schilling L (1987) Change of cerebrovascular reactivity after cortical spreading depression in cats and rats. *Brain Res* 411:72–80

Wienhard K, Dahlbom M, Eriksson L, Michel C, Bruckbauer T, Pietrzyk U, Heiss WD (1994) The ECAT EXACT HR: performance of a new high resolution positron scanner. *J Comput Assist Tomogr* 18:110–118

Woods RP, Iacoboni M, Mazziotta JC (1994) Bilateral spreading cerebral hypoperfusion during spontaneous migraine headache. *N Engl J Med* 331:1689–1692

Journal of Clinical Neuroscience (2002) 9(2), 187–189

DOI: 10.1054/jocn.2001.1006, available online at http://www.idealibrary.com on IDEAL®

Radiology study

Hyperintense MCA branch sign on FLAIR-MRI

Masatoshi Koga MD, **Kazumi Kimura** MD, **Kazuo Minematsu** MD, **Takenori Yamaguchi** MD

Cerebrovascular Division, Department of Medicine, National Cardiovascular Center, 5-7-1 Fujishirodai, Suita, Osaka 565-8565, Japan

Summary We report three patients with cardioembolic stroke or transient ischaemic attack. Fluid-attenuated inversion recovery (FLAIR) MRI within hours of symptom onset, demonstrated linear hyperintensities on the surface of the cortex corresponding to neurologic deficits. This unusual finding was indicative of MCA branch occlusion that was confirmed or suggested with angiography. Ultra-early evaluation with FLAIR- and diffusion-MRI may help establish the diagnosis of acute ischaemic stroke particularly due to embolic MCA branch occlusion.

Keywords: cardioembolic stroke, magnetic resonance imaging, fluid-attenuated inversion recovery, middle cerebral artery

INTRODUCTION

Fluid-attenuated inversion recovery (FLAIR) magnetic resonance imaging (MRI) can detect cortical ischaemic lesions more accurately than T2 or T1 weighted MRI,[1] because FLAIR-MRI improves contrast between the signal intensity of a strong T2 weighted image of brain parenchyma and suppressed signal intensity of the adjacent cerebrospinal fluid. However, it does not reliably demonstrate ischaemic lesions within hours after stroke onset. Recent technological developments have enabled us to detect hyperacute ischaemic lesions by diffusion weighted imaging (DWI), which allows a more sensitive and specific evaluation of ischaemic lesions than conventional MRI.[2]

We report herein three patients with hyperacute ischaemic stroke or TIA by embolic occlusion of the middle cerebral artery (MCA) branches. In these patients, FLAIR images taken within hours after stroke onset revealed linear hyperintensities, indicative of MCA branch occlusion. This finding, hyperintense MCA branch sign, may be useful in the diagnosis of MCA branch occlusion even within hours of stroke onset, and help to begin appropriate treatment promptly.

SUBJECTS AND METHODS

The three patients were admitted to our hospital within 2.5 hours after stroke onset. Immediately after routine neurological and computer tomographic (CT) examinations, they underwent MRI. The MRI examination was performed on a 1.5 Tesla system (MAGNETOM Vision, Siemens) equipped with single-shot echo-planar imaging (EPI). The MRI studies included axial FLAIR and DWI sequences. The slice thickness was 4 mm, and the interslice gap was 2 mm. For the FLAIR images the acquisition parameters were as follows: repetition time (TR) 9000 msec, echo time (TE) 105 msec, inversion time 2400 msec, 182 × 256 matrix, field of view (FOV) 173 × 230 mm. DWI were obtained with the following parameters: TR 4000 msec, TE 100 msec, 96 × 200 matrix, FOV 230 × 230 mm.We used two b values (0 and 1000 sec/mm^2). Diffusion gradients were applied in successive scans in each of the x, y, and z directions, and DWI images were formed from the average of these values.

Subsequently, two of the three patients were examined with subtraction cerebral angiography (DSA). In the other patient, cerebral arteries were evaluated with MRA.

FLAIR-MRI were repeated days or weeks after the initial examination in two of the three patients.

Received 2 April 2001
Accepted 25 May 2001

Correspondence to: Masatoshi Koga MD, 2-16-23 Takatori, Sawara-ku, Fukuoka 814-0011, Japan. Tel.: +81-92-843-3138; Fax: +81-92-843-3138; E-mail: mkoga@ff.iij4u.or.jp

CASE REPORTS

Case 1

A 75 year old man with a history of carotid TIA, paroxysmal atrial fibrillation (AF) admitted to our hospital 2.5 hours following sudden onset of right hemiparesis. On admission, his blood pressure was 160/70 mmHg, with an irregular heart rate of approximately 60/min. Neurological examination revealed mild disturbance of consciousness and right hemiparesis. Electrocardiography showed atrial fibrillation. Brain computed tomography (CT) did not demonstrate any fresh lesions in correspondence with the neurologic deficits but rather an old hypodense lesion in the right MCA branch region. DWI revealed a hyperintense area in the left parietal cortex (Fig. 1a). Furthermore, FLAIR showed linear hyperintense structures on the surface of the left temporoparietal cortices (Fig. 1b). Digital subtraction angiography (DSA) was performed five hours after stroke onset, and revealed an occlusion of the left angular artery and poor collateral flow through leptomeningeal anastomoses (Fig. 2). On Day 22, the hyperintense lines were not detected on FLAIR (Fig. 1c). The ischaemic lesion was larger in size as compared to that on the initial DWI. The patient presented with only mild neurologic deficits when discharged home on Day 30.

Case 2

A 57 year old man with a history of acute hepatitis was admitted due to sudden onset of right hemiparesis. On admission, his blood pressure was 138/78 mmHg, with a regular heart rate of 72/min. His neurologic deficits resolved within one hour, and the diagnosis of transient ischaemic attack (TIA) was made. On the following day (Day 2), his heart rhythm changed from sinus to AF followed by consciousness

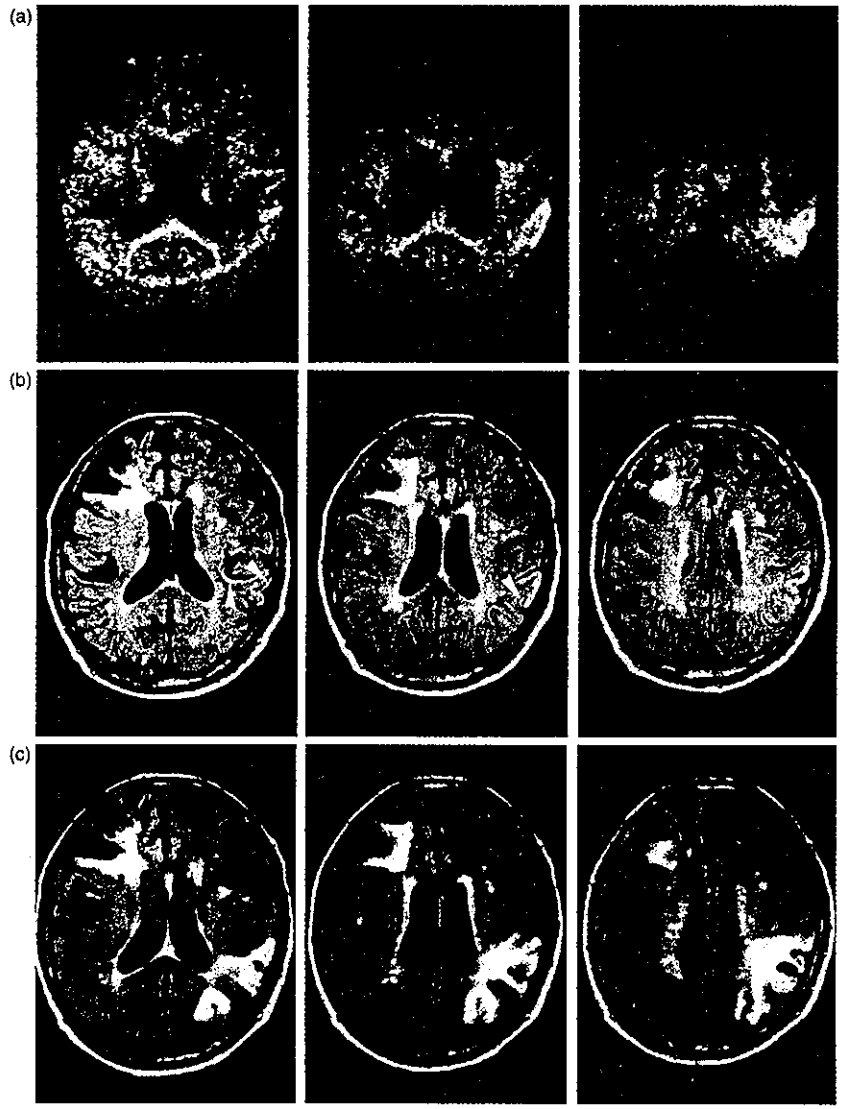

Fig. 1 MRI studies in patient 1. DWIs taken at 3.5 hours after stroke onset demonstrates high intensity areas in the left angular artery region (a). FLAIR images show linear high intensities (arrowheads) in the region of the MCA branch (b). In FLAIR images 22 days post onset, the linear hyperintesity is not observed (c).

disturbance, aphasia and right hemiparesis two hours later. One hour after the onset of these symptoms, DWI showed a hyperintense lesion in the left MCA insular region. FLAIR revealed a linear hyperintensity on the surface of the corresponding cortex (Fig. 3a). DSA revealed an occlusion of the left MCA branches and poor collateral flow. The linear hyperintensity was not visualised on the 2nd FLAIR examination on Day 8. He was transferred to a rehabilitation hospital with a moderate hemiparesis and aphasia on Day 68.

Case 3

A 30 year old woman with hypertrophic cardiomyopathy and non-sustained ventricular tachycardia was admitted to our hospital for a caesarean section. Three days postpartum, she suddenly developed aphasia and left side hemiparesis. Her blood pressure was 120/70 mmHg, with a regular heart rate of 70/min. Three hours after symptom onset, DWI revealed a hyperintense lesion in the left MCA region. FLAIR demonstrated a linear hyperintensity on the surface of the corresponding cortex (Fig. 3b). MR angiography (MRA) showed that horizontal segments of the bilateral MCA were patent, but the left MCA branches looked hypovascular compared with the right ones. The patient's neurologic deficits resolved completely within 24 hours.

DISCUSSION

The present three patients were diagnosed as having cardioembolic stroke (Case 1 and 2) or TIA (Case 3). Embolic MCA branch occlusion was confirmed with DSA in two patients, and was suggested with MRA in the other patient. Hyperacute DWI examinations detected early ischaemic lesions that might expand later as shown in Case 1. Hyperacute FLAIR-MRI could not visualise early ischaemic brain

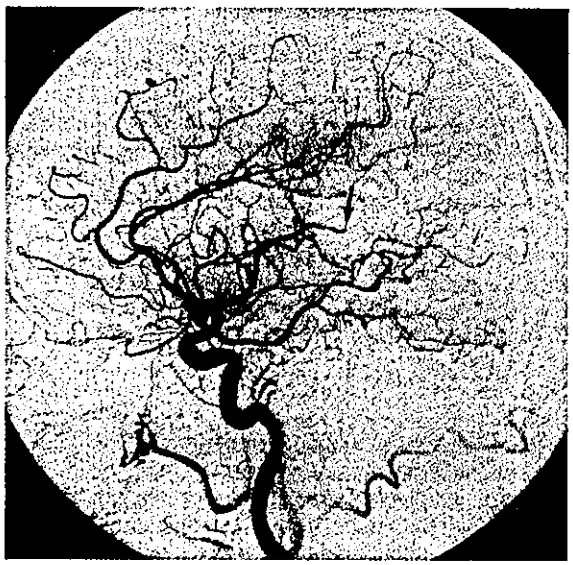

Fig. 2 Left carotid angiogram (lateral view) in patient 1. An occlusion of the left MCA angular artery is demonstrated (arrow).

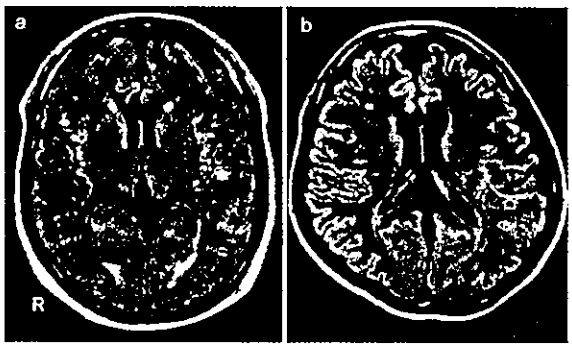

Fig. 3 A FLAIR image in patient 2 (a). The image was obtained 1 hour after symptoms onset. A liner high intensity is demonstrated (solid arrow). A FLAIR image in patient 3 (b). The image was obtained 3 hours after stroke onset. A linear high intensity corresponding to a branch of MCA is visualised (open arrow).

damage, but demonstrated linear hyperintensities on the surface of the corresponding cortex, indicative of MCA branch occlusion. We termed this unusual finding a 'hyperintense MCA branch sign'. MRA and transcranial Doppler ultrasound can detect arterial occlusive lesions only in the proximal intracranial arteries, but not in the distal ones. Therefore, in hyperacute ischaemic stroke, FLAIR-MRI may be a valuable method to noninvasively evaluate MCA branch occlusion.

Gács et al. reported CT visualisation of acute intracranial arterial occlusions, especially trunk occlusions of the MCA.[3] The finding was labeled the 'hyperdense MCA sign', and has been used in an instant diagnosis of embolic MCA occlusion. The diagnostic sensitivity of this sign, however, is low as it is present in only 40–60% of patients with angiographically proven occlusion of the MCA.[4,5]

Noguchi et al. recently reported that, in nine of 11 patients with complete proximal MCA occlusion, the distal portion of the MCA was visible as a linear hyperintense signal on FLAIR images.[6] The arterial hyperintense signal on FLAIR images was explained by very slow retrograde collateral flow due to leptomeningeal anastomosis, as revealed by angiography. Moreover, a fresh thrombus in the artery may also produce the hyperintense signal on FLAIR images. The hyperintense MCA branch sign in our cases was perhaps caused by a fresh thrombus because collateral flow revealed by DSA was poor. Similar vascular hyperintensity on FLAIR-images may be detected in patients with distal arterial occlusion in other vascular territories.

The hyperintense appearance on FLAIR-MRI may relate to several factors, including the effects on both T1 and T2 relaxation that were discussed in patients with subarachnoid haemorrhage and cerebral intraventricular haemorrhage.[7–10] The FLAIR technique produces strong T2-weighted images that are highly sensitive to T2 prolongation. T2 prolongation may result from a high protein content[8–10] and a rich oxyhaemoglobin.[8] We think that these conditions of fresh thrombus in stasis may play a role in hyperintense appearance on FLAIR-MRI.

The treatment with recombinant tissue plasminogen activator is beneficial for hyperacute ischaemic stroke. Rapid and noninvasive evaluation of vascular and brain lesions is essential for appropriate treatment of hyperacute ischaemic stroke. According to the present results, the hyperintense MCA sign on FLAIR-MRI may be a useful diagnostic sign, particularly when combined with DWI.

REFERENCES

1. Brant-Zawadzki M, Atkinson D, Detrick M, Bradley WG, Scidmore G. Fluid-attenuated inversion recovery (FLAIR) for assessment of cerebral infarction. Initial clinical experience in 50 patients. Stroke 1996; 27: 1187–1191.
2. Warach S, Gaa J, Siewert B, Wielopolski P, Edelman RR. Acute human stroke studies by whole brain echo planar diffusion-weighted magnetic resonance imaging. Ann Neurol 1995; 37: 231–241.
3. Gács G, Fox AJ, Barnett HJM, Vinuela F. CT visualization of intracranial arterial thromboembolism. Stroke 1983; 14: 756–762.
4. Bastianello S, Pierallini A, Colonnese C, Brughitta G, Angeloni U. Hyperdense middle cerebral artery CT sign. Comparison with angiography in the acute phase of ischemic supratentorial infarction. Neuroradiol 1991; 33: 207–211.
5. von Kummer R, Meyding-Lamadé U, Forsting M et al. Sensitivity and prognostic value of early CT in occlusion of the middle cerebral artery trunk. AJNR Am J Neuroradiol 1994; 15: 9–15.
6. Noguchi K, Ogawa T, Inugami A et al. MRI of acute cerebral infarction: a comparison of FLAIR and T2-weighted fast spin-echo imaging. Neuroradiol 1997; 39: 406–410.
7. Noguchi K, Ogawa T, Inugami A, et al. Acute subarachinoid hemorrhage: MR imaging with fluid-attenuated inversion recovery pulse sequences. Radiology 1995; 196: 773–777.
8. Bradley WG. MR appearance of hemorrhage in the brain. Radiology 1993; 189: 15–26.
9. Melhem ER, Jara H, Eustace S. Fluid-attenuated inversion recovery MR imaging: identification of protein concentration thresholds for CSF hyperintensity. AJR Am J Roentgenol 1997; 169: 859–862.
10. Bakshi R, Kamran S, Kinkel PR et al. Fluid-attenuated inversion-recovery MR imaging in acute and subacute cerebral intraventricular hemorrhage. AJNR Am J Neuroradiol 1999; 20: 629–636.

Effects of Anticoagulation on Infarct Size and Clinical Outcome in Acute Cardioembolic Stroke

Masayuki Wakita, MD, Masahiro Yasaka, MD, Kazuo Minematsu, MD, and Takenori Yamaguchi, MD, *Osaka, Japan*

Effects of anticoagulation on infarct size and outcome have not been fully elucidated in patients with acute cardioembolic stroke, although the anticoagulation therapy reduces both occurrence and recurrence of ischemic stroke greatly. The authors retrospectively investigated the relationship of anticoagulation intensity to infarct size and outcome. In 104 consecutive patients (mean age 70.8 ±10.0 years) who had suffered acute supratentorial cardioembolic infarction or transient ischemic attacks, they analyzed risk factors for atherosclerosis, underlying heart diseases, the infarct size (maximal area) on brain computed tomography, and modified Rankin scale score upon discharge. They compared these clinical data between patients who had received warfarin before the ictus and those who had not. In addition, they investigated the effects of the international normalized ratio (INR) on infarct size and outcome in 19 patients who had been receiving anticoagulant therapy and had measurement of INR within 24 hours after stroke onset. There were 25 patients who had received anticoagulation before the stroke (A/C group) and 79 patients who had not (non-A/C group). The infarct size in the A/C group tended to be smaller than that in the non-A/C group ($p = 0.081$, Mann-Whitney U test). In the 19 patients who had prior anticoagulation and measurement of INR within 24 hours of stroke onset, large infarcts were seen in 6 of 13 patients with INR < 1.6 and in none of 6 patients with INR ≥ 1.6. Poor clinical outcome was observed in 5 patients with INR < 1.6, but in none with INR ≥ 1.6. In conclusion, anticoagulant therapy with INR ≥ 1.6 appears to effectively prevent a large infarct and poor outcome, even when ischemic stroke dose occurs in patients with an emboligenic heart disease.

Introduction

Anticoagulation using warfarin reduces the risk of ischemic stroke in patients who have an emboligenic heart disease.[1] Five prospective randomized clinical trials in patients with nonvalvular atrial fibrillation (NVAF) have identified the safety and efficacy of anticoagulation for stroke prevention.[2-6] These trials showed that anticoagulation reduces occurrence of ischemic stroke by nearly 70% compared to the rate in untreated patients.[7] According to collaborative analysis of these trials, the risk factors for ischemic stroke in NVAF patients were determined to be history

Angiology 53:551–556, 2002

From the Cerebrovascular Division, Department of Medicine, National Cardiovascular Center, Osaka, Japan

This study was supported in part by research grants for Cardiovascular Disease (9A-8, 12A-2, 12C-1) from the Ministry of Health and Welfare of Japan

Correspondence: Masahiro Yasaka, MD, Cerebrovascular Division, Department of Medicine, National Cardiovascular Center, 5-7-1 Fujishirodai, Suita, Osaka, 565-8565, Japan
E-mail: yasakam@hsp.ncvc.go.jp

of previous stroke or transient ischemic attack (TIA), diabetes mellitus, hypertension, advanced age, congestive heart failure, and ischemic heart disease.[8,9] In NVAF patients aged 75 years or younger who have such risk factors of stroke, warfarin therapy with a target International Normalized Ratio (INR) of 2.0–3.0 is recommended for primary prevention of stroke.[7,10] Low-intensity warfarin therapy, however, was reported to be safer than conventional intensity therapy in elderly people.[11] The lower limit of the low-intensity warfarin therapy has not been determined yet.

In patients with acute cardioembolic stroke, the effects of anticoagulation on infarct size and clinical outcome have not yet been sufficiently evaluated. Hence, we retrospectively investigated whether the administration of warfarin before stroke onset produced a favorable effect on infarct size and clinical outcome in patients with acute cardioembolic stroke, and we discuss the lower limit of effective anticoagulation.

Methods

We investigated 110 patients who were admitted to our hospital consecutively between January 1996 and April 1999 owing to acute supratentorial cardioembolic stroke or TIA. The diagnosis of cardioembolic stroke was made according to the criteria reported by Yamaguchi et al[11] and Minematsu.[12] The patient group consisted of 69 men and 41 women, mean age 70.1 ±10.4 years. We excluded from this study 5 patients who underwent intraarterial thrombolytic therapy and 1 patient with prior anticoagulant therapy who presented massive hemorrhagic infarction (hematoma type) on admission. Data of the remaining 104 patients (65 men and 39 women, mean age 70.8 ±10.0 years) were retrospectively analyzed for the purpose of this study.

We classified the 104 patients into 2 groups: 25 patients who had received anticoagulant therapy before the ictus (A/C group) and the remaining 79 patients who had not (non-A/C group). The following demographic data were compared between the 2 groups; (1) age and gender; (2) risk factors for stroke, including hypertension, diabetes mellitus, hyperlipidemia, smoking habits, and alcohol consumption; (3) history of brain infarction; (4) a score of the National Institutes of Health Stroke Scale (NIHSS) assigned upon admission[13]; and (5) underlying heart diseases confirmed by electrocardiography and transthoracic or transesophageal echocardiography. We determined the maximal area of the infarct on a computed tomographic (CT) scan taken after the first week of stroke as an infarct size. The infarct size was classified arbitrarily as either small (< 10 cm^2) or large (≥ 10 cm^2), and clinical outcome upon discharge was evaluated by the modified Rankin scale.[14] We compared the size of infarct and outcome at discharge between the 2 groups.

The definitions of the risk factors were as follows: (1) hypertension, use of antihypertensive agents, systolic blood pressure > 160 mm Hg or diastolic blood pressure > 95 mm Hg; (2) diabetes mellitus, use of oral antihyperglycemic agents, insulin, or glycosylated hemoglobin (HbA_{1C}) $> 6.4\%$; and (3) hyperlipidemia, use of antihyperlipidemic agents or a fasting serum total cholesterol level > 220 mg/dL.

The intensity of anticoagulation was expressed as the INR determined by use of thromboplastins of low international sensitivity index values.[15,16] Additionally we analyzed the relationship of the INR value to infarct size and outcome in patients who had been receiving anticoagulant and had INR measurement within 24 hours of stroke onset.

Data are expressed as the mean ± sd or median and range. The frequency of each risk factor was compared between the 2 groups by use of the chi-square test. In the event of low cell counts (< 5), Fisher's Exact Test was used. The nonparametric Mann-Whitney U test was used to evaluate differences in infarct size and modified Rankin scale score, and the unpaired t test was used for the analysis of continuous variables. Statistical analysis was performed using a commercially available software package (Stat-View, version 5.0; SAS Institute, Cary, NC). Statistical significance was established at the $p < 0.05$ level.

Results

No significant difference was found for the frequencies of clinical features, with exceptions of the A/C group including more women (56% vs 32%) and having a more frequent history of cerebral infarction (72% vs 18%) than the non-A/C group ($p < 0.05$ and $p < 0.0001$, respectively) (Table I).